An application of Wavelet analysis to fractal character of Indian Dipole Mode

Zhiyong Huang[1] and Hiroshi Morimoto[2]

[1,2] Graduate School of Environmental Studies, Nagoya University

[1]*Corresponding author's address*: Dr. Zhiyong Huang, Graduate School of Environmental Studies, Nagoya University, Furo-cho, Chikusa-ku, Nagoya 464-8601, Japan.
E-mail: huangmoonsun@yahoo.com

[2]

[1]

ABSTRACT

In this study, short-term climatic transitions within Quasi-Biennial (QB) cycles are considered “noise” for El Niño/Southern Oscillation (ENSO). The noise characteristic is represented by the Hurst coefficient *H*. Fractal dimension analysis and stochastic resonance (SR) are adopted to cope with the roles of noise for ENSO.

The oscillation of *H* of Nino3.4 SST mostly corresponded with the development of El Niño, particularly during two strong Tropical Pacific Decadal Oscillation (TDO) periods of 1894 to 1923 and 1978 to 2000. This represents a stochastic resonance mechanism in the internal Pacific ocean-atmospheric system that is when a positive-phase noise overlaps with a stronger positive-phase TDO, SST easily exceed the critical state to launch an El Niño. This mechanism gives the condition whereby the onset of El Niño is more sensitive to noise.

IOD and noise in DMI (high frequencies of IOD) are two external triggers of ENSO and affect ENSO through the SR mechanism. Phase-lead is an important feature as a trigger in an SR system. When the noise in DMI leads (lags) noise in a Niño3.4 SST, the correlation between IOD and ENSO increases (decreases) after 1910s. SR explains how external noise set out an El Niño. Noise in DMI

influencing ENSO progressively advances from that of DMI, after the 1930s.

1. Introduction

ENSO relates to floods, droughts, typhone, heat wave and other climatical disturbances in a range of locations around the world (e.g. McPhaden et al. 2006). It effects global ecosystem and has socio-economic impacts, especially for the developing countries that are greatly dependent upon their agricultural and fishery sectors for food supply and employment (Tropical Atmosphere Ocean project, TAO).

a. Stochastic resonance and ENSO

Stochastic resonance (SR) (Benzi et al. 1981) is becoming a universal concept in many fields and has proven itself to be remarkably powerful and valid. Through SR one can investigate the impact of noise on a system. The historical SR is classified into four classes. The first class of SR is that an external source has a periodic oscillation that modulated a system, and the system presents a remarkable signal of modulated frequency (Nicolis, 1993). The well-known example is that of the forced harmonic oscillator. The second class of resonance is that the respond frequencies may not be the same as the modulated ones, but would be several times or a sequence of rational fractions of the modulated frequencies (Jin et al. 1994). Thirdly, a continuous banded frequency responds to a continuous banded frequency (Paldor et al. 2000).

Fourth, a certain high frequency causes the system to jump from one state to another state such as warm state of El Niño and cold state of La Niña (Wang et al. 1999). In this study, the fourth case refers to the so-called stochastic resonance.

Essentially, the basic elements for an SR system are a particle, a threshold of energy between the two or more stable states such as ground and excited states, and a trigger which attempts to produce a jumping between two stable states. SR consists of two or more stable states, a trigger, and a jumping (Badzey et al. 2006). The trigger gives an additional forcing to a particle. A jumping happens when the energy of the modulated frequency overlaps the energy of the other frequencies. Both internal periodic forcing and external periodic forcing can be a trigger (Benzi et al. 1981). The importance of a trigger is even a weak external forcing may cause a jumping (Ditlevsen et al. 2005). Moreover, as a trigger, noise can cause and end the resonance (Wang et al. 1999). For a comprehensive review see Gammaitoni et al. (1998).

Basically, El Niño and La Niña are results of resonance in the large interannual climate variations in the Pacific ocean-atmospheric system (Jin et al. 1994). The overlapping of several resonances leads to the chaotic behavior (Jin et al. 1994), and more chaos leads to a stochastic phenomenon (Wang et al.

1999). There are some studies on SR for ENSO, such as Jin et al. (1994) in which earth's annual cycle is a modulation; Tziperman et al. (1994) in which seasonal cycle is a trigger; and Wang et al. (1999) in which wind is a noise resource. These studies are limited to the Pacific zonal resonance. In contrast, the fact that atmospheric resonant modes respond to ENSO can be found in studies such as Wu et al. (2004), Pozo-Vazquez et al. (2005) and Toniazzo et al. (2006).

Previous studies have not documented the resonance mechanism between El Niño/La Niña events and external forcing outside of the Pacific zone such as the Indian Ocean Dipole (IOD, Saji et al. 1999). Instead of a model-based study, a real data-based study has not been carried out.

ENSO events do not co-occur with IOD events (Saji et al. 2003). ENSO and IOD are two interacting systems: for example a strong ENSO and IOD can enhance each other (Saji et al. 2003). Does it mean that IOD may be a trigger for El Niño, and El Niño may be a trigger for IOD? Whether IOD is an "enhancer" or a "trigger" (Chen et al. 2008), the problem is how to confirm phase-lead feature of a trigger, and when it happens. In the following, noise characteristic analysis was used for finding the condition of resonance. A wavelet phase method was required for investigating phase-lead features of

resonance.

b. Noise characteristics and ENSO

The fractal dimension, also known as the Hurst coefficient *H* (first proposed by Hurst, 1951), is important for climate study (Koutsoyiannis, 2006) as it relates to the long-range persistence of the system (Guerrero et al. 2005). *H* is dependent on time-space frequency. Both data-based and model-based studies (for example, Fraedrich et al. 2004) have documented the temporal and spatial fractal dimensions of sea surface temperature (SST). The relationships between the time-frequency dependent *H* for SST and the development of an El Niño event have not been documented so far. The importance and necessity of it are based on the following experiences.

Noise in the ENSO signal refers to high-frequency forcing and small spatial scale processes such as a westerly wind burst or Madden-Julian Oscillation (MJO, 30-60 days cycle). The importance of noise for forecasting El Niño is controversial with some researchers supporting its use (Dijkstra et al. 2002, amongst others), but others not (e.g. Chen et al. 2004).

Additionally, the Tropospheric Biennial Oscillation (TBO; Meehl et al. 1997) greatly affects on ENSO. The Indian Ocean Dipole (IOD, Saji et al. 1999) is mainly due to Quasi-Biennial (QB) cycle and as an aspect of TBO

(Rao et al. 2002), interacting with ENSO (Behera et al. 2006) and influencing on ENSO through the Darwin pressure (Behera et al. 2003). The biennial variability of ENSO is a part of TBO (Li T. et al. 2006). TBO and IOD are important factors for El Niño.

An essential element of any TBO mechanism is the memory of the ocean, and some certain short-term oscillations such as Kelvin wave also contribute to TBO mechanism (Meehl et al. 2003). This TBO mechanism provides us possibilities to explore an index *H* of a short-term memory, which only depends on frequencies within QB, to investigate the noise characteristics of SST accompanying the development of El Niño.

ENSO has a cycle of two to seven years. In this study, short-term climatic transitions that cycles under two years are considered “noise” and cycles longer than seven years are the “background state”. Therefore, *H*, which has restricted frequencies within QB, is used to index the noise characteristics (the mean power of noise) of SST.

This study aims to find the relationship of *H* with the development of an El Niño/La Niña event and the way noise and background interact leading up to the onset of an El Niño event. Stochastic resonance was applied to investigate how noise sets out an El Niño and what conditions for ENSO are sensitive to

noise.

The rest of the paper is organized as follows. Section 2 presents the source of data. Section 3 explains the methods used and explored the index of noise characteristics in investigating the role of noise for ENSO. Section 4 presents the noise characteristics of Nino3.4 SST that is the internal noise in an ENSO system. Section 5 investigates external noise such as IOD and noise in DMI as a trigger for ENSO, where it emphasizes the phase-lead feature of a trigger. Section 6 is a discussion of the paper, with section 8 giving conclusions and suggestions for further work.

2. DATA

a. Niño3.4 SST

The Niño 3.4 region is the area covering (5^0N-5^0S, 120^0W-170^0W). Niño 3.4 SST is one of the most sensitive indices to El Niño events (Hanley et al. 2003).

The Niño 3.4 SST comprises monthly data set from the Hadley Centre Sea Ice and SST Data Set (HadISST), over the period from 1870 to 2005. The data was provided by Hadley Centre, Met Office, UK (Rayner et al. 2003).

b. ENSO event-index

The ENSO event-index is a value representing the intensity of an El Niño/La Niña event for a given year (Severov et al. 2004), which is one of the following (shown in Table 2.1): –1.5 (strong La Niña), –1 (medium strength La Niña), –0.5 (weak La Niña), 0 (neutral year), 0.5 (weak El Niño), 1 (medium strength El Niño), and 1.5 (strong El Niño), respectively. The time series of ENSO event-index from 1870 to 2000 is shown in Fig. 2.1.

c. IOD and DMI

The Indian Ocean Dipple (IOD) (Saji et al. 1999) is the coupled ocean-atmospheric phenomenon evolving with an east-west dipole in the Indian Ocean SST anomaly.

The intensity of the IOD is named as Dipole Mode Index (DMI, Saji et al. 1999). DMI is represented by anomalous SST gradient between the western equatorial Indian Ocean (50^0E-70^0E and 10^0S-10^0N) and the southeastern equatorial Indian Ocean (90^0E-110^0E and 10^0S-0^0N).

The monthly and yearly (averaged from Jan. to Dec.) time series of DMI used in this study can be obtained from the JAMSTEC Frontier Research Center for Global Change (FRCGC) web site (http://www.jamstec.go.jp/frcgc/research/d1/iod/).

3. METHODOLOGY

a. Fractal analysis based on wavelet transform method

A wavelet-based method can accurately estimate the Hurst coefficient *H* (Wang et al. 2003), and is more beneficial than the Fourier-based method (McCoy et al. 1996).

b. Morlet wavelet and Daubechies wavelet

It is important to select a proper wavelet for climate study. Some suggestions of how to select wavelet techniques can be found in the articles written by Torrence and Compo, (1998). In this study, the Morlet wavelet and the second order of the Daubechies orthogonal wavelet have been applied for the different purpose.

Fig. 3.1 shows the smooth and symmetric natures of Morlet wavelet. However, Fig. 3.2 shows the sharp and asymmetric characters of Daubechies wavelet of order 2.

Morlet wavelet is commonly recommended for the climate studies when studying time-frequency partners (Gu et al. 1995). The Morlet wavelet (Fig. 3.1) was applied to investigate the power spectra of a time series.

There has been an increase in application of the Daubechies wavelet for turbulent phenomena, such as typhoons and storms such as Katul (1996). This study applied it in estimating *H*.

c. Daubechies orthogonal wavelet function for estimating H

The second order of the Daubechies orthogonal wavelet function was selected for estimating *H* based on the following reasons.

Firstly, the asymmetric shape of the Daubechies wavelet, shown in Fig. 3.2, matches the idealized skew feature of an El Niño/La Niña episode. The classical delayed oscillator mode (Nagai et al. 1992) of an El Niño/La Niña episode includes the processes that include a long waiting time, the time to evolve to an El Niño event, a quickly cool down to La Niña, and then change to a normal state again. Secondly, an El Niño event exhibits a turbulent signal (or pulse-like event, Yano et al. 2004). The Daubechies wavelet function is suited to a study of turbulent signals (Katul et al. 1996). Lastly, Discrete Wavelet Transform (DWT) takes advantage of forecasting (Torrence and Compo, 1998). A good understanding of the characteristic of discrete wavelet power spectra for SST is significant for in understanding ENSO better and will help us in further forecasting work..

d. Algorithms for estimating H

The Discrete Wavelet Transform, $d_{j,k}(x)$ of a finite-energy signal $f(\cdot)$ of a fractional Brownian motion (fBm) is defined as follows:

$$d_{j,k}(x) = \int f(x) \cdot \psi_{j,k}(x)dx,$$
$$= \int f(x) \cdot 2^{j/2} \psi(2^j x - k)dx, \qquad (1)$$

where $\psi(\cdot)$ is the mother wavelet and $x \in R,\ j,k \in Z$.

Therefore, the estimator $V_b(a)$ (Carmona et al. 1998, Huang et al. 2008) for the Hurst coefficient *H* takes the form:

$$V_b(a) = E\left\{d_{j,k}^2(x)\right\} = C \cdot 2^{-(2H-1)j}, \qquad (2)$$

where C is a constant. The term $E\left\{d_{j,k}^2(x)\right\}$ could be roughly viewed as the averaged energy over the scale of $a = 2^{-j}$.

The logarithm of equation (2) leads:

$$\log_2 E\{d_{j,k}^2(x)\} = -(2H+1)j + \log_2(C), \qquad (3)$$

A linear fitted on the plot of equation (3) yields the slope rate *K* of linear-fitted line, namely $K = -(2H + 1)$. Therefore, the discrete wavelet spectral

estimator for H has the form:

$$H = \frac{-K-1}{2} \qquad (4)$$

where K is the slope rate of linear-fitted line.

The plot of the logarithm of Daubechies wavelet spectra against the logarithms of timescale is called a "log-log plot" (for example, Fig. 3.3) in this paper. For example, selected a segment of the Niño3.4 SST with a period of 64 months starting from January 1997. Then applied the Daubechies wavelet transform for equation (3). Fig. 3.3 shows the log-log plot of 1997 (red curve). The year 1997 had a strong El Niño. The dashed black line is a linear-fitted line for the log-log plot of 1997. From which, one can estimate the H by equation (4).

e. Calculation procedures for generating the time series of H

The following procedure was used to analyze a time series such as the Nino 3.4 SST in this study (Huang et al. 2008):

1. A time window of the SST time series was selected with a period of 64 months, equivalent to the average ENSO cycle, starting from January. The years used for definition of H are supposed to be the start years.

2. The Daubechies wavelet based spectral analysis was applied to the selected SST time window.

3. The Hurst coefficient H was calculated using $H=(K_1-1)/2$, where $K_1 = -K$ is the slope rate of the linear-fitted line of a log-log plot, shown in Fig. 3.3.

4. The time window was then shifted forward one year and the steps 1 to 3 repeated.

In Fig. 3.3, from equation (3), the slope of the log-log plot shows the average energy of wavelet spectra subjected to noise that frequency within QB, and H relates to the slope of the log-log plot. Therefore, H is an index of the mean power of noises.

The Fig. 3.4 shows the time series of noise characteristic index H for Nino3.4 SST, named Hnino34. In this section, Hnino34 is called H. In the section 5, Hnin34 is used.

f. wavelet coherency and phase

The definitions for wavelet coherency and phase are refer to the Torrence et al. (1999) or recent developments Maraun et al. (2007).

For example, Fig. 3.5 shows two random signals of y1 (upper Panel 3.5) and y2 (lower Panel 3.5). The signal y1 leads y2 by 3 months. Fig. 3.6 shows

wavelet coherency (upper Panel 3.6) and phase (lower Panel 3.6) of y1 and y2. In lower Panel 3.6, a positive phase near 0.5*PI on a scale of one year means that y1 leads y2 by (0.5*PI)/(2PI)*1yr=3 months.

4. The role of noise in the Tropical Pacific Ocean for ENSO

In this section, results have been published in Huang et al. (2008) and are summarized as follows.

a. Sensitivity of noise characteristic index H to ENSO

Fig. 4.1 shows the relationship between the oscillations of *H* and that of the ENSO event-index. The shaded areas indicate the same in phase oscillation.

The oscillation of the noise characteristics of Nino3.4 SST, represented by *H,* mostly corresponded with the development of El Niño, meaning that noise corresponded well to the development of an El Niño event, particularly during two significant periods 1894 to 1923 and 1978 to 2000.

b. Stochastic resonance as a possible modulation mechanism

Fig. 4.2 shows the Morlet wavelet spectra for Niño 3.4 SST. During 1894 to 1923 and 1978 to 2000, respectively, there were very energetic oscillations of

the decadal/interdecadal cycle, in other words, strong Tropic Pacific Decadal Oscillation (TDO) signals.

The oscillation of *H,* mostly corresponded with the development of El Niño, particularly during two strong TDO periods of 1894 to 1923 and 1978 to 2000. This represents a stochastic resonance mechanism in the internal Pacific ocean-atmospheric system that when a positive-phase noise overlaps with a stronger positive-phase TDO, SST would easily exceed the critical state to launch an El Niño. This mechanism gives the condition whereby the onset of El Niño is more sensitive to noise.

5. External forcing from Indian Ocean and stochastic resonance

a. IOD as an external trigger for ENSO

IOD interacts with ENSO. It is found that the largest lag correlation coefficient between the monthly Niño3.4 SST and DMI is 0.27 when DMI leads Niño3.4 SST by one month. This implies that IOD may be a trigger for El Niño.

However, the interaction between IOD and ENSO changes period by period. A sliding correlation between an ENSO event-index and yearly DMI (in simple terms, rENSO-DMI) was carried out. Fig. 5.1 shows the sliding correlation

between them, where the length of the sliding window is 10 years. It was found that during the early 1880s and 1900s, 1910s to the 1930s, and after the 1970s, that there were high positive correlations (>0.5). However, some short periods around 1880, early 1940, and 1960 showed negative correlations (<-0.5).

Moreover, in Fig. 5.2, it can be found that most of strong and medium El Niño events show phase co-oscillations between ENSO event-index and DMI, especially after 1970.

These results support previous research that IOD significantly interacts with ENSO (Li et al. 2006). This means that IOD may be a trigger of resonance for El Niño/La Niña.

Without the effect of ENSO, IOD is mainly due to the QB cycle (Behera et al. 2006). Therefore, interest naturally concerns the role of noise in DMI. The noise in DMI is discussed in the following subsections.

b. Noise characteristics in DMI

To investigate the noise characteristics in DMI, the fractal analysis method (see section 3.4) is applied for time series of DMI. Therefore, the time series of Hdmi is calculated and shown in Fig. 5.3.

c. Noise in DMI as an external trigger for ENSO

Noise in DMI plays a significant role for the onset of El Niño and La Niña. To investigate the difference in the role of noise in DMI and DMI itself for ENSO, sliding correlations was carried out between the ENSO event-index and Hdmi (the black curve in Fig. 5.4, in simple terms, rESNO-Hdmi), and compared it to rENSO-DMI (red-dotted curve in Fig. 5.4). The length of sliding window is 10 years.

From Fig.5.4, it can be found that the phase oscillations are similar between them after 1910, and the phase of rENSO-Hdmi leads phase of rENSO-DMI after the 1930s. This means that noise in DMI plays an important role for ENSO, and implicates that noise in DMI influencing ENSO progressively advances from that of DMI, though noise in DMI is a part of DMI. This result supports the previous study of Behera et al. (2003). Noteworthy, the phase oscillation of rENSO-Hdmi is similar to the inter-decadal change in the IOD-Darwin correlation that was documented by Behera et al. (2003).

Do these mean that the interactions between noise in DMI and ENSO may overtake DMI? If not, when does noise in DMI lead DMI to interact with ENSO? In the next subsection, wavelet phase is used for investigation.

d. Wavelet phase and phase-lead of a modulator

The wavelet coherency between Niño3.4 SST and monthly DMI is shown in

Panel 5.5(a) and wavelet phase is shown in Panel 5.5(b). In Panel 5.3(a), a significant level above 95 percent is shown in frequency from two to eight years during 1920 and 1940. There are a little weaker coherency periods in the periods from 1870 to 1880, 1975 to 2000.

The puzzle is why during 1920 and 1940 significant wavelet coherency is shown in cycles of two to eight years, since both Niño3.4 SST and DMI are weak in this period (wavelet power spectra of them are not shown here). This question is left for further investigation.

The wavelet phase is shown in Panel 5.3(b). The positive value means that Niño3.4 SST leads DMI, as shown by blue and pink parts. The negative value means that DMI leads Niño3.4 SST, as shown by the green, yellow and red parts. It can be found that most of cycles smaller than eight years show that DMI leads Niño3.4 SST (green, yellow and red parts). This means that on average, DMI leads ENSO. This result meets the canonical correlation analysis (in section 5.1) that DMI leads ENSO for one month by which there is a significantly large lag correlation coefficient of 0.27.

To investigate the role of noise in DMI for ENSO, the wavelet phase between them within the QB cycle was carefully investigated. It can be found that noise in DMI leads noise in Niño3.4 SST in some periods such as 1890 to

1910 (except 1903 and 1914), 1950 to 1960, and 1965 to 2000 (except 1979 and 1981).

In Fig. 5.6, by carefully comparing the sliding correlation of rENSO-Hdmi with wavelet phase within QB cycles, it is found that when noise in DMI leads Niño3.4 SST, the correlation increases, that when noise in DMI lags Niño3.4 SST, the correlation decreases. This means that noise in DMI is a trigger for Niño3.4 SST, and so noise in DMI is a trigger for El Niño/La Niña events.

To confirm this finding, by investigating the relationship between the monthly time series of Niño3.4 SST and DMI, it can be seen that most of DMIs lead La Niña, and some strong El Niño events lead IOD (figures not shown here). These findings imply that noise in IOD is a trigger for El Niño/La Niña events.

6. DISCUSSION

The overlapping of two or more nonlinear resonances leads to the chaotic behavior (Jin et al. 1994), and more Chaotic behaviors will result in stochastic behavior (Wang et al. 1999). Fractal dimension is an index of long-range persistence of a stochastic system (Guerrero et al. 2005). This research puts

forward in understanding when and how noises set out an El Niño event. This study has investigated the role of noise for ENSO through fractal analysis and stochastic resonance (SR). These methods developed pave a new road in the research on noise.

Firstly, fractal analysis was applied to investigate the noise characteristics of ENSO. The results are robust with respect to statistical significance tests, showing the dim activity of ENSO during the 1920s -1970s due to the weak contribution of the TDO cycle. The previous studies show that the time series of ENSO indices manifested a regime shift around 1978, found initially by Quinn et al. (1985). The importance of this feature may be relates to interdecadal climate variability over the North Pacific and Parts of North America (Graham et al. 1994), global warming (Zhang et al. 1997), the Pacific Decadal Oscillation (PDO, Mantua et al. 1997), and TDO (Fedorov et al. 2000). The causes and mechanisms of TDO climate changes are extratropical-tropical teleconnections by means of fast atmospheric bridges (Barnett et al. 1999), and slow meridional overturning circulation in the upper ocean (Gu et al. 1997), but remain not fully understood (see Miller et al. 2000 for a review). The topic of teleconnection between decadal/interdecadal climate variability and ENSO require further study.

Secondly, an SR system includes a threshold of energy between two stable states, a trigger, and a jumping. This study puts forward that phase-lead is an important feature as a trigger in an SR system. High frequencies or short-term climatic transitions play a phase-lead feature in the trigger for ENSO. Noise characteristics analysis of the tropical Pacific Ocean shows that noise in Nino3.4 SST is a trigger for ENSO. For further confirmation of the role of noise for ENSO with IOD is an important external forcing, noise in the Indian Ocean was investigated. From wavelet phase analysis and sliding correlation analysis, it can be found that not only IOD but also noise in DMI was a trigger for ENSO. The results support the previous studies that IOD can be a trigger of ENSO (Behera et al. 2003).

IOD and ENSO are two independent systems (Saji et al. 1999). IOD leads ENSO in certain cases (Behera et al. 2003) and in the other cases ENSO leads IOD (Behera et al. 2006). IOD may be triggered by ENSO (Behera et al. 2006) during certain years (Saji et al. 2003). By investigating the relationship between the monthly time series of Niño3.4 SST and DMI, it can be seen that most IODs lead La Niña. Some strong El Niño events lead IOD. A more comprehensive discussion on the mechanisms of how IOD and ENSO enhancing each other can be found in the previous study by Saji et al. (2003). Worthwhile triggers can not only can set out but also end a resonance, such as MJO and Asian Monsoon,

and they can set out an El Niño, and can end an El Niño. These cases studies are lacking in the present research.

What the exact critical state is in an SR system is still an unresolved question, that is, how a particle jumps from one stable state to another stable state. The question must be left for future study using either a physical explanation or a statistical one.

7. CONCLUSION AND FURTHER WORK

Noise represents short-term climate transitions whose frequency is within QB, including MJO, the Kelvin wave, the Rossby wave, QBO, IOD, Asian Monsoon, TBO, and so on. Noise is important when studying climate. It can start an El Niño, and can end an El Niño. In certain periods, El Niño is sensitive to noise whereas in other periods, it is not. The roles of noise for ENSO are significant but not yet clear. When can it start or end an El Niño? How does it start an El Niño? Are there certain general modes or conditions for noise to trigger an El Niño? This study has adopted wavelet-based fractal dimension analysis to explore the noise index H, and used SR to identify when an external noise such as IOD triggers an ENSO dynamic, and emphasized phase-lead feature of a trigger. This would be beneficial for understanding the role of noise

for ENSO and would be used for improving the method of forecasting ENSO.

The main findings of this study are summarized as follows:

The oscillation of the noise characteristics, represented by *H*, which was frequency-dependent within QB, mostly corresponded with the development of El Niño, particularly during 1894 to 1923 and 1978 to 2000. This was due to the contribution of strong signals of the TDO background. A stronger TDO background provides the conditions for high frequencies to be more efficient to the onset of an El Niño. This represents a stochastic resonance mechanism in the internal Pacific ocean-atmospheric system. When a positive-phase noise overlaps with a stronger positive-phase TDO, SST easily exceeds the critical state to launch an El Niño, and gives the conditions when the onset of El Niño is more sensitive to noise.

The threshold of energy between two states, a trigger, and a jumping are three elements of an SR system. Phase-lead is an important feature for a trigger in an SR system. Noise has an effect on ENSO through a stochastic resonance mechanism. IOD and noise in DMI are two triggers for ENSO.

When noise in DMI leads Niño3.4 SST, the correlation increases, however, when noise in DMI lags Niño3.4 SST, the correlation between IOD and ENSO decreases. This means that noise in DMI is a trigger for a Niño3.4 SST, namely,

IOD is a trigger for El Niño/La Niña events. SR explains how external noise can trigger an El Niño.

The way that El Niño and La Niña affect the short-term memory of the ocean interacting with TBO or IOD requires further investigation. What is the critical state of a particle jumping form one stable state to another stable state, either in a physical explanation or in a statistical one? Can they be represented them in the time-frequency space? These questions must be left for further study.

This study put forward the role of noise for ENSO. The methods could be used for improving the methods for forecasting ENSO. More attention should be paid to the broader ENSO-related SR and teleconnections, and the exact critical points of spectrum variation both in SR are not yet clear. These issues are currently under investigation.

8. REFERENCES

Ausloos M, 2004: Statistical physics in meteorology, *Phys. A* **336,** 93-101.

Badzey R. L., and P. Monhanty, 2006: Coherent signal amplification in a nanomechanical oscillator via stochastic resonance. *AIP Confernece Proceedings* **850**,1675-1676.

Barnett T. P., D. W. Pierce, M. Latif, D. Dommenget, and R. Saravanan, 1999: Interdecadal interactions between the tropics and midlatitudes in the Pacific basin. *Geophys. Res. Lett.* **26**, 615–618.

Behera S. K., and T. Yamagata, 2003: Notes and Correspondence. Influence of the Indian Ocean dipole on the Southern Oscillation. *J. Meteoro. Soc. Japan* **81**, 169-177.

Behera S. K., J. J. Luo, S. Masson, S. A. Rao, H. Sakuma, and T. Yamagata, 2006: A CGM Study on the Interaction between IOD and ENSO. *J. Climate* **19,** 1688-1705.

Benzi R., A. Sutera, and A. Vulpiani, 1981: Letter to the editor. The mechanism of stochastic resonance. *J. Phys. A: Mathematical and Theoretical* **14**, L453-L457.

Carmona R., W. L. Hwang, and B. Torresani, 1998: Practical Time-Frequency

Analysis: Gabor and Wavelet Transforms with an Implementation in S. In *Wavelet Analysis and Its Applications* **9,** Charles K. Chui, (eds). Academic Press.

Chen D., M. A. Cane, A. Kaplan, S. E. Zebiak, and D. Huang, 2004: Predictability of El Niño over the past 148 years. *Letters to Nature* **428**, 733-736.

Chen D., and M. A. Cane, 2008: El Niño prediction and predictability. *J. Computat. Phys.* **227**, 3625-3640.

Dijkstra H. A., and G. Burgers, 2002: Fluid Dynamics of El Niño Variability. *Ann. Rev. Fluid Mech.* **34,** 531-558.

Ditlevsen P. D., M. S. Kristensen, and K. K. Andersen, 2005: The recurrence time of Dansgaard–Oeschger Events and limits on the possible periodic component. *J. Climate* **18,** 2594-2603.

Fedorov A, and S. G. H. Philander, 2000: Is El Niño changing? *Science* **288**, 1997.

Fraedrich K., U. Luksch, and R. Blender, 2004: 1/f model for long-time memory of the ocean surface temperature. *Phys. Rev. E* **70**, 037301.

Gammaitoni, L. P., P. J. Hanggi, and F. Marchesoni, 1998: Stochastic resonance. *Rev. Mod. Phys.* **70**, 223–287.

Graham N. E, 1994: Decadal-scale climate variability in the 1970s and 1980s:

Observations and model results. *Climate Dyn.* **10**, 135–162.

Gu D., and S. G. H. Philander, 1995: Secular changes of annual and interannual variability in the tropics during the past century. *J. Climate* **8**, 864-876.

Gu D., and S. G. H. Philander, 1997: Interdecadal climate fluctuations that depend on exchange between the tropics and extratropics. *Science* **257**, 805–807.

Guerrero A., and L. A. Smith, 2005: A maximum likelihood estimator for long-range persistence. *Phys. A* **355**, 619-632.

Hanley D. E., M. A. Bourassa, J. J. O'Brien, S. R. Smith, and E. R. Spade, 2003: A Quantitative evaluation of ENSO indices. *J. Climate* **16**, 1249-1258

Huang Z., and H. Morimoto, 2008: Wavelet based fractal analysis of El Niño/La Niña episodes. *Hydrol. Res. Lett.* **2**, 70-74. DOI: 10.3178/HRL.2.70. (http://www.jstage.jst.go.jp/browse/HRL).

Hurst H. E., 1951: Long-term storage capacity of reservoirs. *Trans. Am. Soc. Civ. Eng.* **116**, 770-808.

Jin F-F., J. D. Neelin, and M. Ghil, 1994: El Niño on the Devil's staircase: Annual subharmonic steps to chaos. *Science* **264**, 70-72.

Katul, G., and B. Vidakovic, 1996: The partitioning of attached and detached eddy

motion in the atmospheric surface layer using Lorentz wavelet filter. *Bound.-Layer Meteor.* **77,** 153-172.

Koutsoyiannis D, 2006: A toy model of climatic variability with scaling behavior. *J. Hydrol.* **322**, 25-48.

Li T., P. Liu, X. Fu, B. Wang, and G. A. Meehl, 2006: Spatiotemporal Structures and Mechanisms of the Tropospheric Biennial Oscillation in the Indo-Pacific Warm Ocean Regions. *J. Climate* **19**, 3070-3089.

Mantua N. J., S. R. Hare, Y. Zhang, J. M. Wallace, and R. C. Francis, 1997: A Pacific interdecadal climate oscillation with impacts on salmon production. *Bull. Amer. Meteor. Soc.* **78**, 1069-1079.

Maraun D., J. Kurths, and M. Holschneider, 2007: Nonstationary Gaussian processes in wavelet domain: Synthesis, estimation, and significance testing. *Phys. Rev. E* **75**, 016707.

Meehl G. A., 1997: The south Asian monsoon and the tropospheric biennial oscillation. *J. Climate* **10**, 1921-1943.

Meehl G. A., J. M. Arblaster, and J. Loschnigg, 2003: Coupled ocean-atmosphere dynamical processes in the tropical Indian and Pacific Oceans and the TBO. *J. Climate* **16**, 2138-2158.

Meyers G., P. McIntosh, L. Pigot, and M. Pook, 2007: The Years of El Niño, La Niña, and interactions with the Tropical Indian Ocean. *J. Climate* **20**, 2872-2880.

McCoy E. J., and A. T. Walden, 1996: Wavelet analysis and synthesis of stationary long-memory processes. *J. Comput. Graphical Stat.* **5**, 26-56.

McPhaden M. J., S. E. Zebiak, and M. H. Glantz. 2006. ENSO as an integrating concept in earth science. *Sci*. **314**, 1740-1744.

Miller A., and N. Schneider, 2000: Interdecadal climate regime dynamics in the North Pacific Ocean: theories, observation and ecosystem impacts. *Progr. Oceanogr.* **27**, 257.

Nagai T., T. Tokioka, M. Endoh, and Y. Kitamura, 1992: El Niño-Southern Oscillation simulated in an MRI Atmosphere-Ocean coupled general circulation model. *J. Climate* **5,** 1202-1233.

Nicolis C., 1993: Long-term climatic transitions and stochastic resonance. *J. Stat. Phys.* **70**, 1-14.

Paldor N., and Y. Dvorkin, 2000: Noise-induced interhemispheric particle transport-stochastic resonance in a Hamiltonian system. *J. Atmos. Sci*. **57**, 150-157.

Pozo-Vazquez, D., S. R., Gamiz-Fortis, J. Trovar-Pescador, M. J. Esteban-Parra, and Y. Castro-Diez, 2005: El Niño-Southern Oscillation events and associated

European winter precipitation anomalies, *Int. J. Climatol.* **25**, 17– 31.

Quinn W. H., and V. T. Neal, 1985: Recent long-term climate change over the eastern tropical and subtropical Pacific and its ramifications. *Proc. Ninth Annual Climate Diagnostic Workshop,* Corvallis, OR, NOAA, 101–109.

Rao S. A., S. K. Behera, Y. Masumoto, and T. Yamagata, 2002: Interannual subsurface variability in the tropical Indian Ocean with a special emphasis on the Indian Ocean dipole. *Deep-Sea Res.* **49**, 1549-1572.

Rayner, N. A., 2003: Global analyses of sea surface temperature, sea ice, and night marine air temperature since the late nineteenth century. *J. Geophys. Res.* **108**, DOI: 1029/2002JD002670.

Saji N. H., B. N. Goswami, P. N. Vinayachandran, and T. Yamagata, 1999: A dipole mode in the tropical Indian Ocean. *Nature* **401**, 360-363.

Saji N. H., and T. Yamagata, 2003: Structure of SST and surface wind variability during Indian Ocean Dipole Mode events: COADS observations. *J. Climate* **15**, 2735-2751.

Severov D. N., E. Mordecki, and V. A. Pshennikov, 2004: SST anomaly variability in southwestern Atlantic and El Niño/Southern Oscillation. *Adv. Space Res.* **33,** 343-347.

Toniazzo T., and A. A. Scaife, 2006: The influence of ENSO on winter North Atlantic climate. *Geophys. Res. Lett.* **33**, L24704. doi: 10.1029/2006GL027881

Torrence C., and G. P. Compo, 1998: A practical guide to wavelet analysis. *Bull. Amer. Meteor. Soc.* **79**, 61-78.

Tziperman E., L. Stone, M. A. Cane, and H. Jarosh, 1994: El Niño chaos: Overlapping of resonances between the seasonal cycle and the Pacific Ocean-atmosphere oscillator. *Science* **264**, 72-74.

Wang A. L., C. X. Yang, and X. G. Yuan, 2003: Evaluation of the wavelet transform method for machined surface topography I: methodology validation. *Tribol. Int.* **36,** 517-526.

Wang B., A. Barcilon, and Z. Fang, 1999: Stochastic dynamics of El Niño-Southern Oscillation. *J. Climate* **56**, 5-23.

Wu A., and W. W. Hsieh, 2004: The nonlinear Northern Hemisphere winter atmospheric response to ENSO. *Geophys. Res. Lett.* **31**, L02203. doi:10.1029/2003GL018885.

Yano J. I., R. Blender, C. Zhang, and K. Fraedrich, 2004: 1/f noise and pulse-like events in the tropical atmospheric surface variabilities. *The Quart. J. Roy. Meteor. Soc.* **130,** 1697-1721.

Zhang Y., J. M. Wallance, and D. S. Battisti, 1997: ENSO-like interdecadal variability: 1900-93. *J. Climate* **10**, 1004-1020.

FIGURE CAPTIONS

FIG. 2.1. Time series of ENSO even-index from 1870 to 2000. The value above zero shows the intensity of El Niño, and below zero shows the intensity of La Niña.

FIG. 3.1. The shape of the Morlet wavelet.

FIG. 3.2. The shape of the Daubechies wavelet of order 2.

FIG. 3.3. The log-log plots for the strong El Niño year 1997, and its linear-fitted line (dashed black line). The height of top-right point of the log-log plot corresponds to the average wavelet power spectrum on a scale of QB (32 months).

FIG. 3.4. Time series of *H* for Nino3.4 SST from 1870 to 2000, named Hnino34.

FIG. 3.5. The upper and lower panels show two random signals of y1 and y2 respectively. The signal y1 leads y2 by 3 months.

FIG. 3.6. The wavelet coherency and phase of y1 and y2. In Panel b, the positive phase (blue and pink) means that y1 lead y2.

FIG. 4.1. The time series of *H* and the ENSO event-index. The shaded parts show matching oscillation patterns in phase, especially from 1894 to1923 and 1978 to 2000, shown in detail in the lower two panels.

TABLE 2.1. The ENSO event-indices responded to the intensity of El Niño/La Niña events.

Type	El Niño events			Neutral	La Niña events		
Intensity	Strong	Medium	Weak	Neutral	Weak	Medium	Strong
ENSO event-indices	+1.5	+1.0	+0.5	0	-0.5	-1.0	-1.5

FIGURES

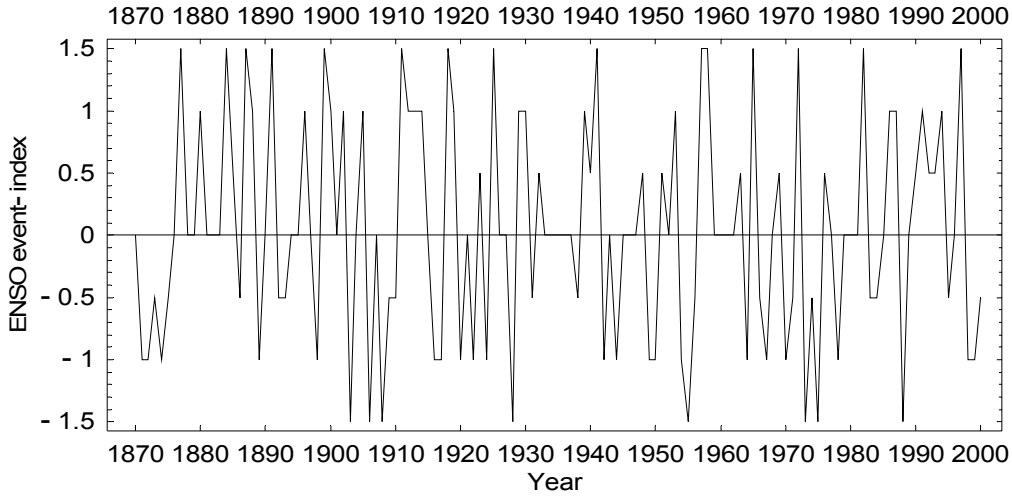

FIG. 2.1. Time series of ENSO even-index from 1870 to 2000. The value above zero shows the intensity of El Niño, and below zero shows the intensity of La Niña.

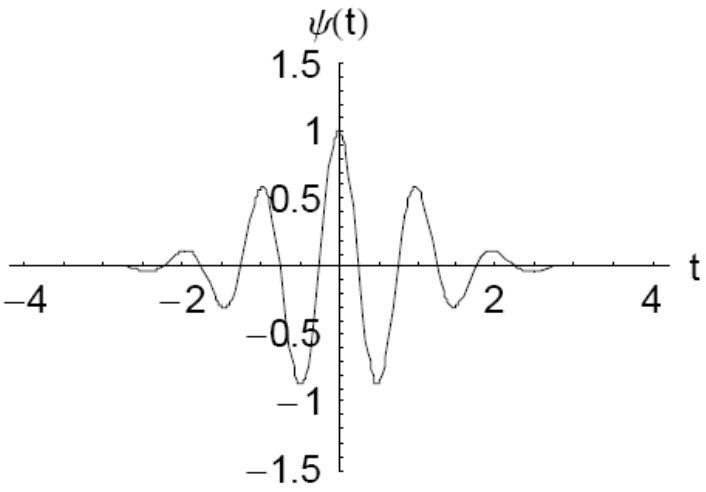

FIG. 3.1. The shape of the Morlet wavelet.

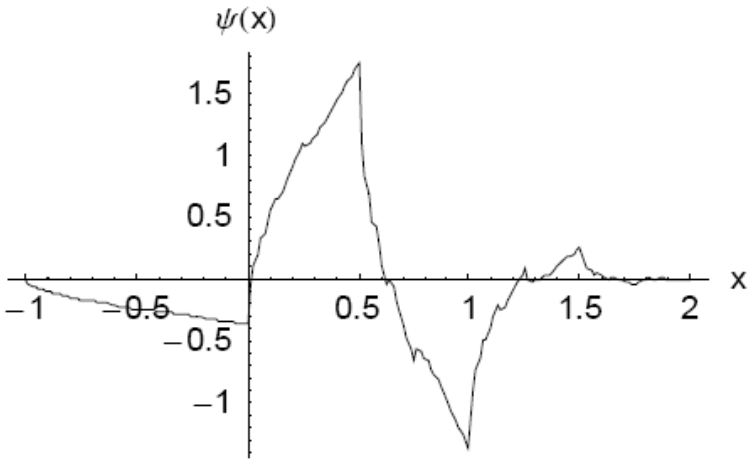

FIG. 3.2. The shape of the Daubechies wavelet of order 2.

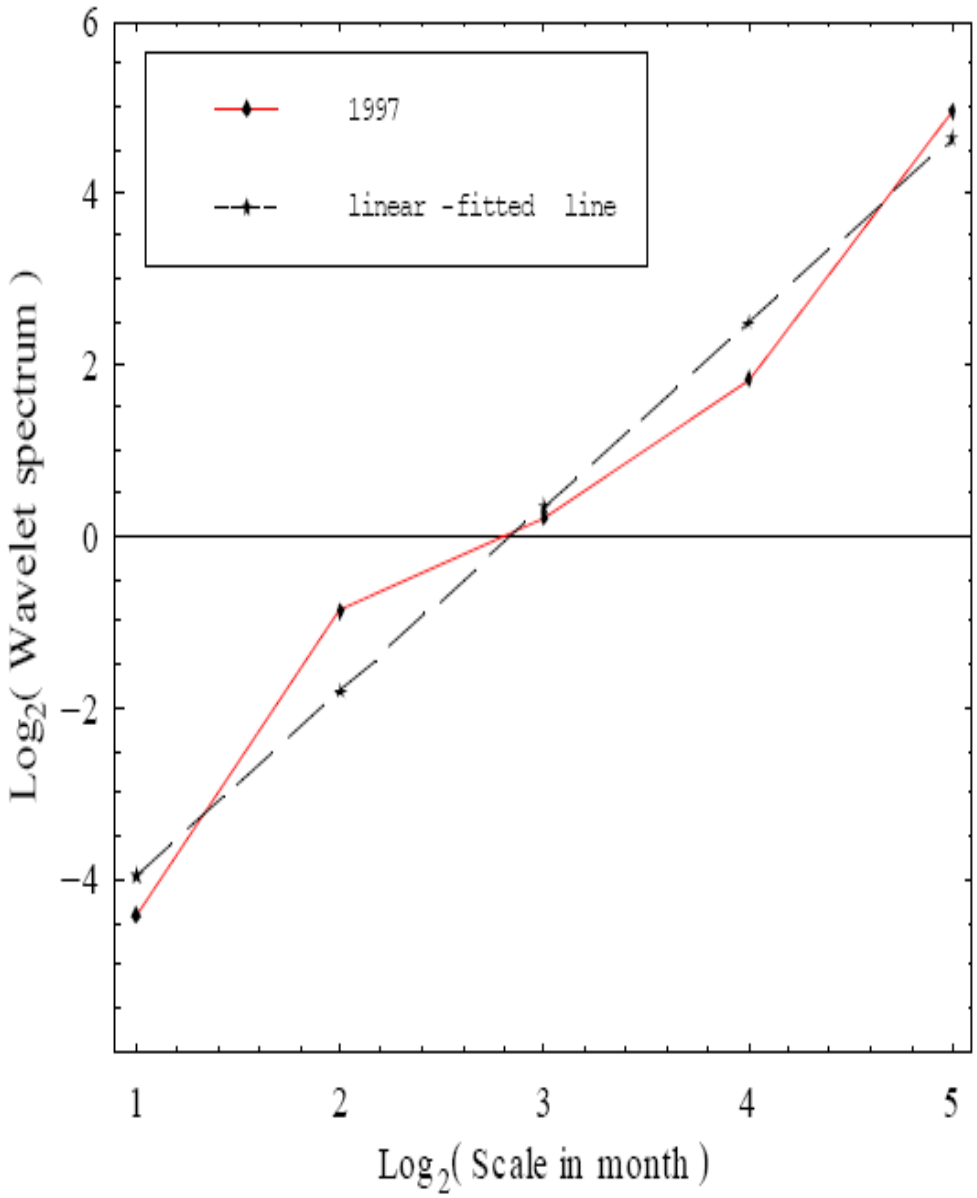

FIG. 3.3. The log-log plots for the strong El Niño year 1997, and its linear-fitted line (dashed black line). The height of top-right point of the log-log plot corresponds to the average wavelet power spectrum on a scale of QB (32 months).

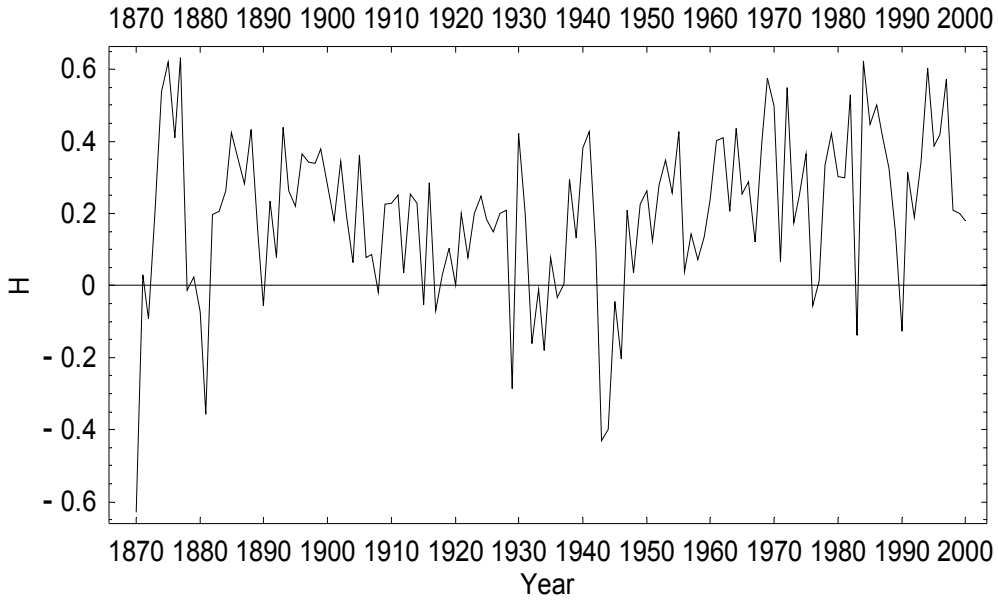

FIG. 3.4. Time series of *H* for Nino3.4 SST from 1870 to 2000, named Hnino34.

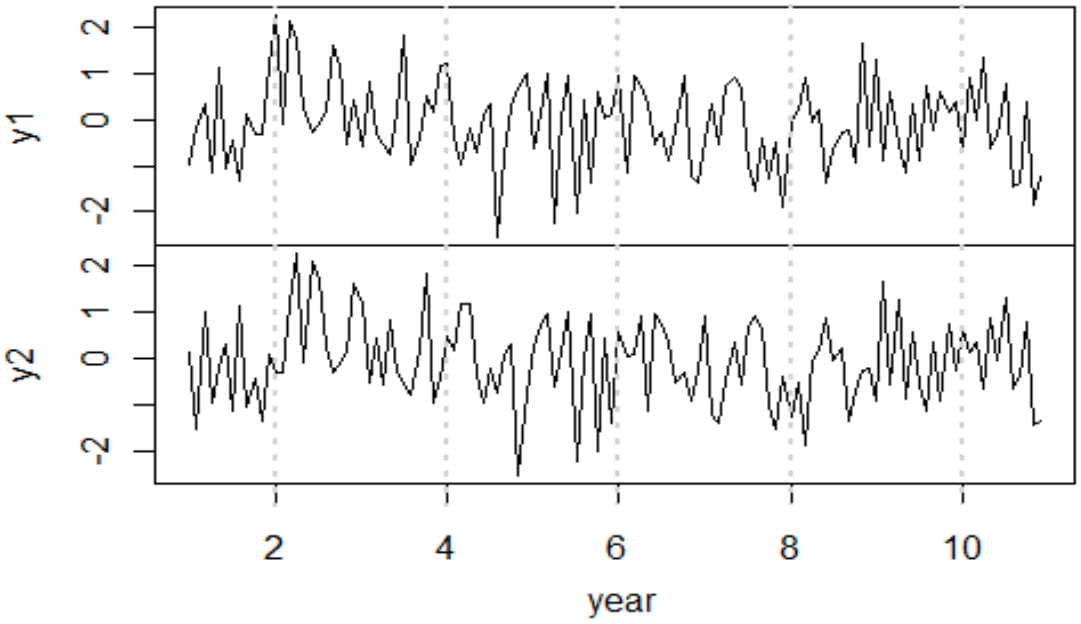

FIG. 3.5. The upper and lower panels show two random signals of y1 and y2 respectively. The signal y1 leads y2 by 3 months.

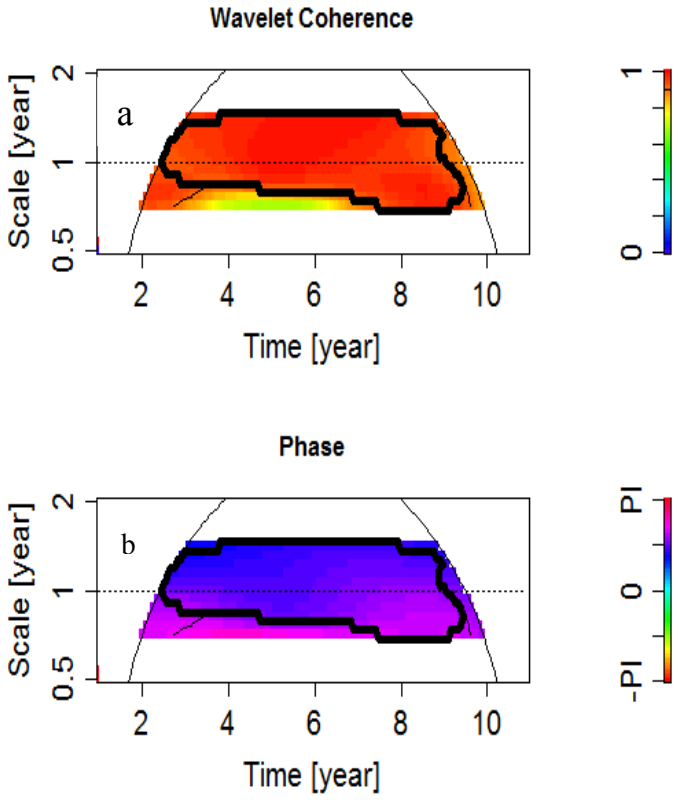

FIG. 3.6. The wavelet coherency and phase of y1 and y2. In Panel b, the positive phase (blue and pink) means that y1 lead y2.

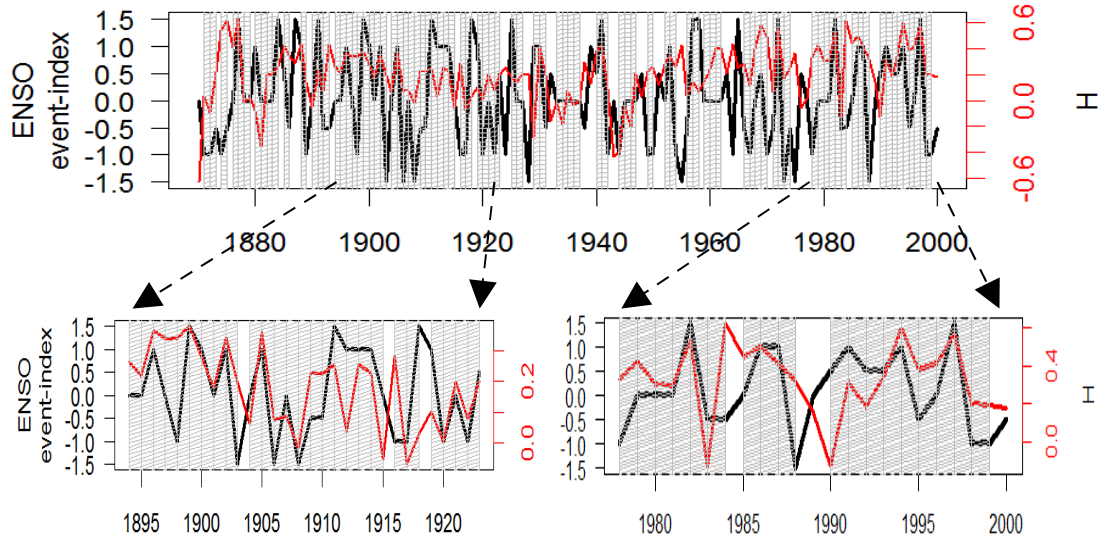

FIG. 4.1. The time series of H and the ENSO event-index. The shaded parts show matching oscillation patterns in phase, especially from 1894 to1923 and 1978 to 2000, shown in detail in the lower two panels.

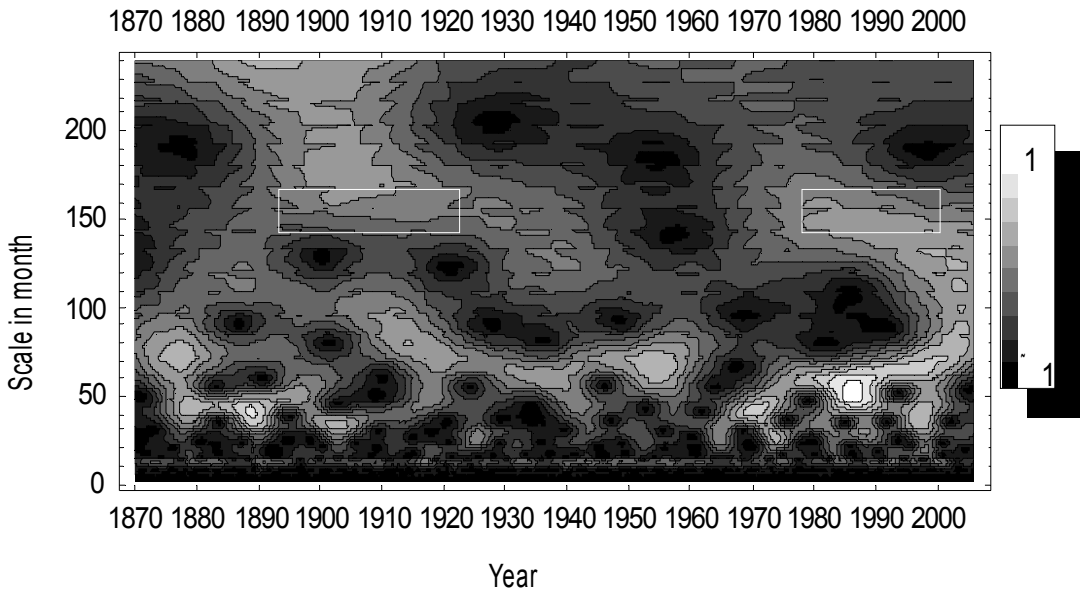

FIG. 4.2. Morlet wavelet spectrum for Niño3.4 SST from 1870 to 2005. The two boxes show two periods of active TDO signals during 1894 to1923 and 1978 to 2000.

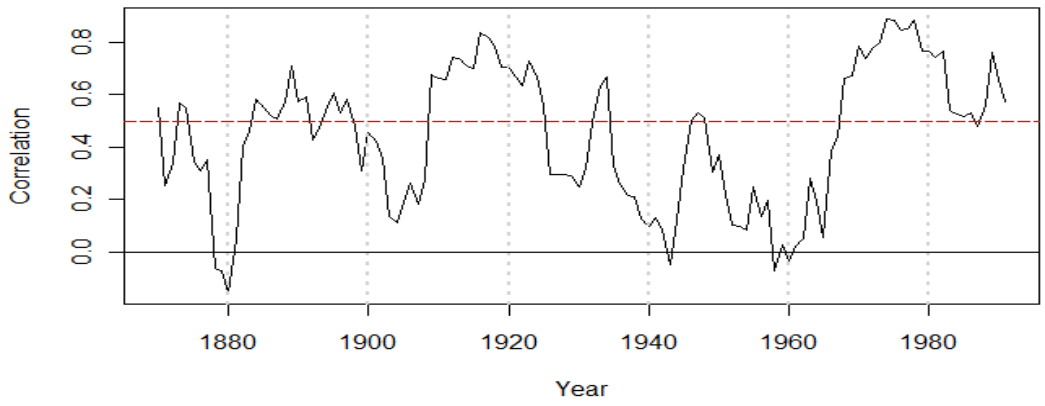

FIG. 5.1. Sliding correlation coefficients between yearly DMI and ENSO event-index (rENSO-DMI). The length of sliding window is 10 years.

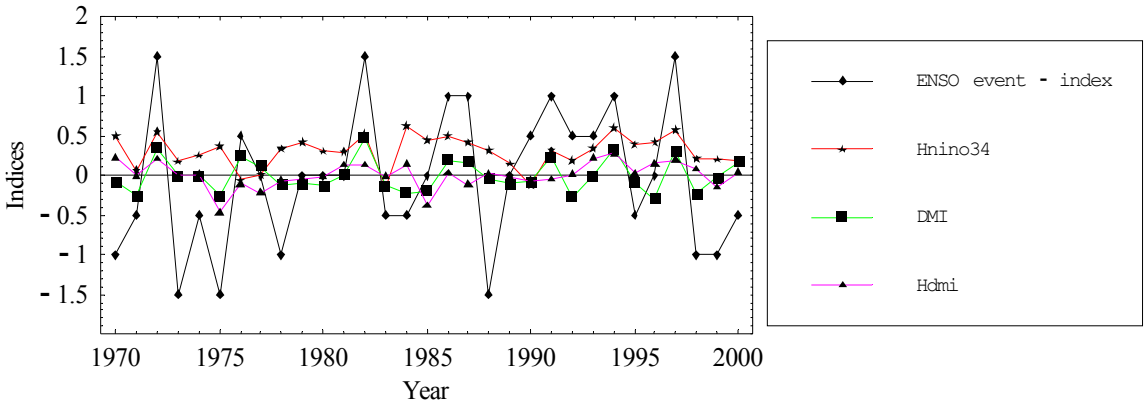

FIG. 5.2. Time series of ENSO event-index (black curve), DMI (green curve), Hnino3.4 (red curve, see section 3.5) and Hdmi (pink curve, see section 5.2).

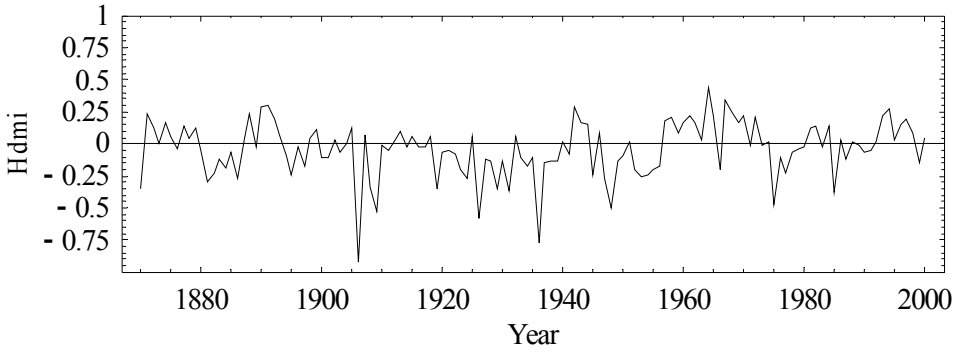

FIG. 5.3. The time series of Hdmi.

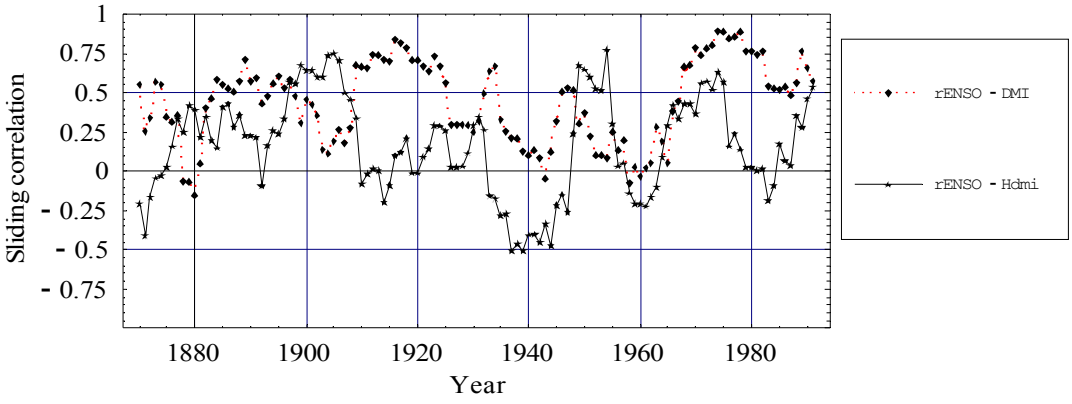

FIG. 5.4. Sliding correlation coefficients between yearly DMI and ENSO event-index (rENSO-DMI), and between Hdmi and ENSO event-index (rENSO-Hdmi). The length of sliding window is 10 years.

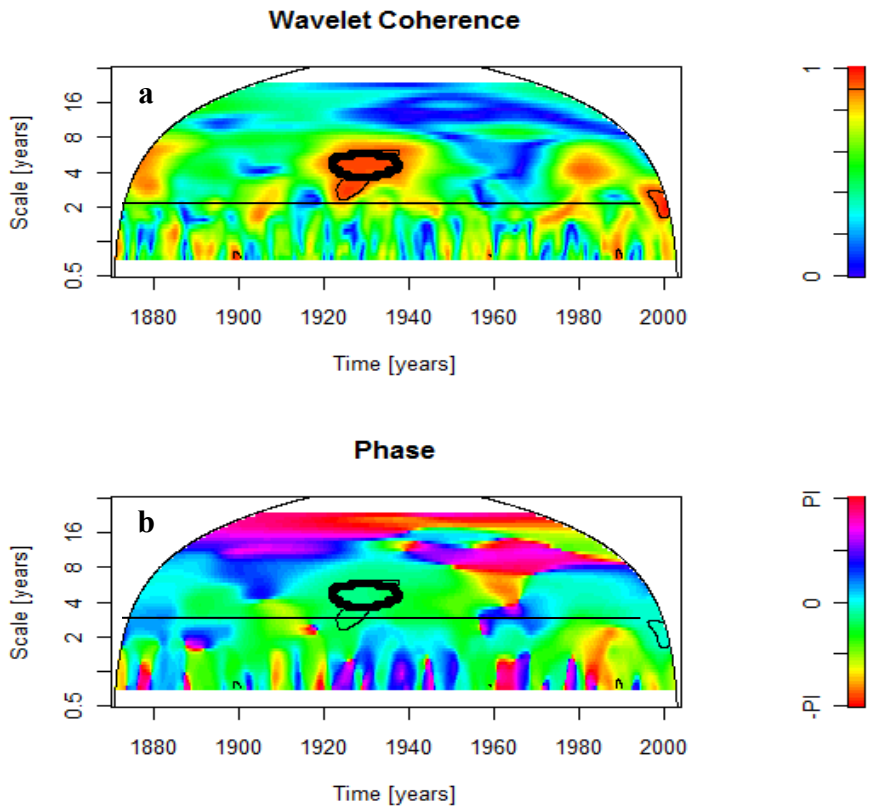

FIG. 5.5. Wavelet coherency (using the Morlet wavelet, Panel (a)) between Niño3.4 SST and DMI and their wavelet phase (Panel (b)). In Panel (a), the thick black contour is the 5% significance level. In Panel (b), the positive value means that Niño3.4 SST leads DMI shown by the blue and pink parts. The negative value means that DMI leads Niño3.4 SST shown by green, yellow and red parts.

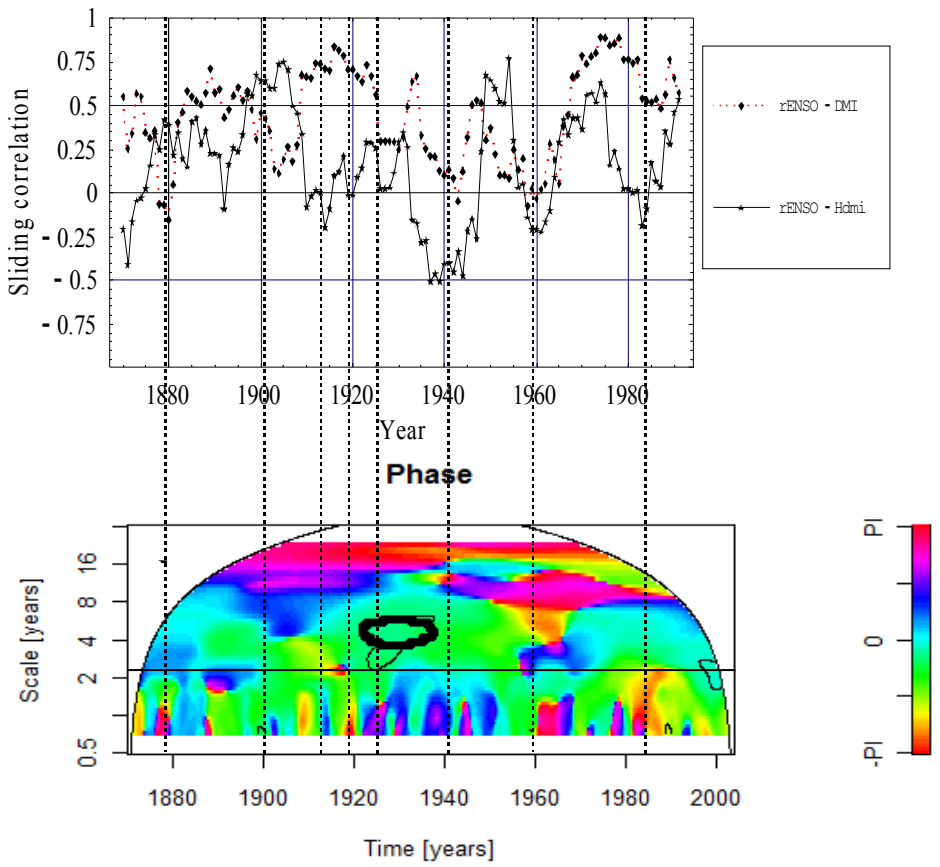

FIG. 5.6. Wavelet phase (lower panel) and sliding correlations of rENSO-DMI and rENSO-Hdmi (upper panel). Dotted lines show some points on which noise in DMI lags Nino3.4 SST and rENSO-DMI is decreasing.